Many-body effects in the quasi-one-dimensional magnetoplasma

M. Bayer, Ch. Schlier, Ch. Gréus, and A. Forchel
Technische Physik, Universität Würzburg, Am Hubland, D-97074 Würzburg, Germany

S. Benner and H. Haug
Institut für Theoretische Physik, Universität Frankfurt, Robert-Mayer-Straβe 8-10, D-60325 Frankfurt/Main, Germany
(Received 28 July 1995; revised manuscript received 9 December 1996)

We compare measured and calculated luminescence spectra of quantum wires in normal magnetic fields. The experiments have been performed on modulated barrier $In_{0.13}Ga_{0.87}As/GaAs$ quantum wires in magnetic fields up to $B=10.5$ T. In the regime of high magnetic fields in which the cyclotron energy ω_c exceeds the lateral intersubband energy Ω the carriers show the behavior of a fully quantized system. The experimental magnetoluminescence spectra for different excitation intensities are in excellent agreement with calculated spectra. The calculations contain not only the influence of the strong magnetic field, but also the many-body effects on a Hartree-Fock level in terms of state filling, band-gap renormalization, and excitonic correlations with up to four lateral subbands. A magnetic-field-dependent momentum cutoff is introduced, which ensures that electrons and holes are not pushed out of the quantum wire under the influence of the Lorentz force. By fitting the calculated to the measured spectra we determine the density and the temperature in the one-dimensional magnetoplasma. In contrast to the field-free case ($B=0$) the renormalization of one subband is mainly determined by the occupation of the other subbands in the high-field regime because the excitons on one subband form, to a good approximation, an ideal gas. Its formation becomes possible because the symmetry under continuous rotations in the electron and hole isospin space that is broken by the lateral confinement is to a good approximation restored by high magnetic fields, which suppress the motion of the free carriers along the wire. [S0163-1829(97)04719-X]

I. INTRODUCTION

Novel nanofabrication techniques permit the production of quasi-one-dimensional semiconductor quantum wires, which have attracted considerable interest because of their size-dependent physical properties and because of their potential for technological applications. These nanostructures have been investigated by quasistationary optical spectroscopy (i.e., by cw measurements) both without[1–4] and with magnetic fields.[5–8] However, many-body effects in these systems have not been studied experimentally as intensely as in systems of higher dimensionality. One of the macroscopic effects of the many-body interactions is the shift of the band-gap to lower energies, the band-gap renormalization.

Without the influence of a magnetic field, the band-gap renormalization in quantum wires has been studied in single and multisubband situations.[9–17] In Refs. 9 and 10 it has been shown that in the absence of a magnetic field the effect of screening on the optical spectra and on the subband gap shifts of quantum wires is relatively small. While in three-dimensional (3D) bulk crystals the ionization of the exciton originates from screening effects, these effects are no longer sufficient to ionize the exciton in 2D quantum wells. In this case, phase-space filling has to be taken into account. In 1D quantum wires the ionization of the exciton solely by phase-space filling is an appropriate description.[9]

Therefore we suggested using a Hartree-Fock description of the Coulomb interactions in quantum wires. Most important is, however, that all Coulomb interactions, namely, the electron-electron, hole-hole, and electron-hole interactions, are treated on the same footing.[11] The first two interactions give rise to self-energy corrections, while the attractive electron-hole interaction introduces the excitonic correlations. The self-energy corrections manifest themselves in a plasma-density-dependent shrinkage of the intersubband gaps, while the excitonic correlations give rise to a strong redistribution of the oscillator strength. At low excitation levels nearly all the oscillator strength is concentrated in one very strong exciton line with a large exciton binding energy. The excitonic ''Sommerfeld factor'' suppresses completely the divergence of the single-particle density of states. With increasing plasma density this exciton emission is transformed continuously into a plasma emission, in which excitonic effects still redistribute oscillator strength away from the band edge to the spectral region above the combined Fermi level. This smooth effect at elevated plasma temperatures is a remanant of the Fermi-edge singularity or of the Mahan exciton at low temperatures. Any unbalanced use of the repulsive carrier-carrier interaction and of the equally strong attractive electron-hole interaction leads to systematic errors in the interpretation of the spectra.

In Refs. 12–14 experimental results of the band-gap renormalization at $B=0$ are discussed within a very simplified picture. For example, the attractive electron-hole interaction is completely neglected by using a free-carrier transition model for the line-shape analysis in order to get information on the band-gap shifts. As expected from such an oversimplified analysis, the results are controversial. In Ref. 14 no band-gap shift at all is found, while in Ref. 13 the band-gap shift obtained with a free-carrier transition model is found to agree to the rather accurate random phase ap-

proximation (RPA) self-energy calculations of Refs. 15 and 16.

A balanced analysis becomes increasingly important as the dimensionality is lowered by quantum confinement. While, e.g., excitonic effects on the optical spectra of a 3D GaAs plasma are still relatively small, so that the errors with a free-carrier transition line-shape analysis are also relatively small, the excitonic effects become even at room temperature much stronger in 2D quantum wells and become really dominant in 1D quantum wires, so that the use of free-carrier transition models in low-dimensional structures, and particularly 1D quantum wires, is not possible.

Consistently analyzed experiments and calculations show clearly that without a magnetic field the plasma-density–dependent shifts of the various lateral subbands depend mainly on the population of the corresponding subband itself.[10] This can be attributed to the small Coulomb intersubband matrix elements. With magnetic fields, to the best of our knowledge, no studies of many-body effects in quasi-one-dimensional systems have been reported up to now.

In this paper we report measurements and calculations of (quasistationary) magneto-optical spectra of quantum-well wires subject to a magnetic field B perpendicular to the quantum-well layer in which the wires are embedded. One important criterion for the quality of the quantum wires is the observation of well-resolved higher lateral subbands. For the quantum wires investigated in the present experiments we have studied the lateral subband structure by high excitation photoluminescence and photoluminescence excitation spectroscopy at $B=0$.[3] In these references the systematic dependence of the energies of the lateral subband transitions on the wire width were shown.

Our previous theoretical work on the magneto-optical properties of quantum wires[17] is extended from only one optically excited subband to a multisubband case. In a parabolic confinement potential the effect of a magnetic field oriented perpendicular to the quantum-well plane on the single-particle energies and wave functions can be calculated exactly. The Coulomb interactions between the carriers, which are assumed to be thermally distributed in their corresponding subbands, are treated consistently in the Hartree-Fock approximation. We include thus several lateral quantum wire subbands, a magnetic field of arbitrary strength, self-energy corrections, and excitonic correlations in a simple but balanced way. In addition to Ref. 17 we take into account in the calculations that the one-dimensional momenta are restricted by the condition that the carriers have to stay within the wire potential under the influence of the Lorentz force. With this procedure the calculated luminescence spectra are in excellent agreement with spectra measured on modulated barrier $In_{0.13}Ga_{0.87}As/GaAs$ quantum wires in magnetic fields up to $B=10.5$ T. We find that in a neutral quasi-one-dimensional magnetoplasma, in contrast to the case of $B=0$, the renormalization of one subband is almost independent of its population but is mainly determined by the population of the other subbands.

This paper is organized as follows. In Sec. II we give a short description of the investigated samples and of the experimental setup that we used to perform magnetophotoluminescence studies. We present luminescence spectra for varying values of the magnetic field strength and for various optical excitation powers. In Sec. III the theoretical model is described, which has been used in order to calculate absorption and luminescence spectra and to show the excitation power dependence of the energies of the observed transitions. In Sec. IV we compare experimental and theoretical spectra and discuss the plasma-density-dependent line shifts. In Sec. V we finally summarize our results.

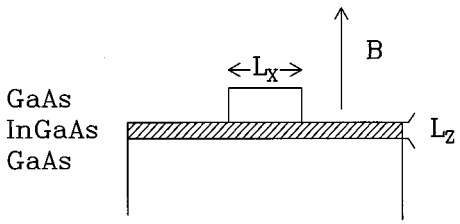

FIG. 1. Schematic sketch of the modulated barrier wires investigated in the present experiments. Also the choice of the coordinate system is shown: The z direction is chosen to be parallel to the quantum-well growth direction and the y direction is parallel to the quantum wires. The magnetic field B was aligned along the z direction.

II. EXPERIMENT

A. Investigated samples and experimental setup

We have investigated the photoluminescence of highly excited modulated barrier $In_{0.13}Ga_{0.87}As/GaAs$ quantum wires with a width of 29 ± 3 nm in magnetic fields up to $B=10.5$ T. These structures have been fabricated by electron beam lithography and by wet chemical etching on a 5-nm-wide quantum well. The heterostructure parameters have been chosen in order to have only one confined electron quantum-well subband, from which the lateral subbands arise by the patterning. A schematic sketch of the wires is shown in Fig. 1. The GaAs top barrier layer of the quantum well has been removed on both sides of the wire by the etching process.[3] This lateral pattern results in different positions in energy of the ground-state quantum-well subbands because the potential profile along the growth direction is, to a good approximation, symmetric in the unetched regions, while it is asymmetric in the etched regions. Therefore the band edges in the etched regions have higher energies than in the unetched regions and hence also in the lateral direction a potential discontinuity is generated that confines electrons and holes in the same spatial regions beneath the remanants of the quantum-well cap layer. The total lateral confinement potential in the modulated barrier structures is about 25 meV, which is comparable to the sum of the electron and hole cyclotron energies $\hbar\omega_c$ at the highest applied magnetic fields of $B=10.5$ T. As mentioned above, the electronic subband structure in these quasi-one-dimensional systems has been studied by photoluminescence and photoluminescence excitation spectroscopy at $B=0$.[3]

The samples have been immersed in liquid helium ($T=1.8$ K) in an optical magnetocryostat ($B\leqslant10.5$ T). As indicated in Fig. 1, the experiments have been performed in Faraday configuration, i.e., the magnetic field has been oriented normal to the quantum well and therefore also normal to the quantum wire axis. A cw Ar^+ laser ($\lambda=514.5$ nm)

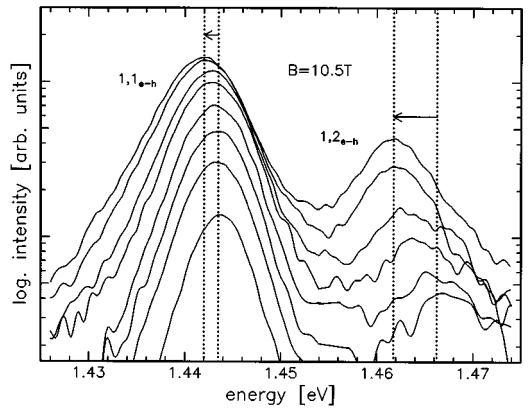

FIG. 2. Experimental luminescence spectra of modulated barrier $In_{0.13}Ga_{0.87}As/GaAs$ quantum wires with a lateral width of 29 nm for various excitation intensities at $B=10.5$ T. The emission intensities are shown on a logarithmic scale. The arrows indicate the shift of the spectral lines between the spectrum recorded with minimum excitation power and the spectrum recorded with maximum excitation power.

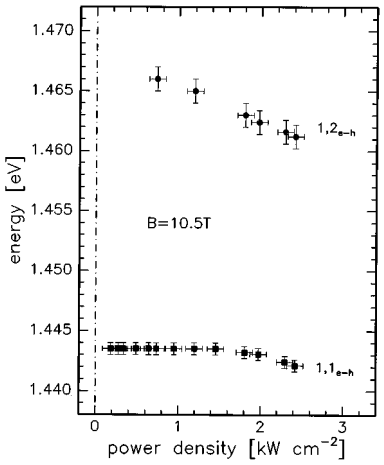

FIG. 3. Transition energies at $B=10.5$ T observed for the 29-nm-wide $In_{0.13}Ga_{0.87}As/GaAs$ quantum wires as functions of the excitation power densities that were used to record the corresponding spectra.

has been used for optical excitation with power densities of up to 3 kW cm^{-2}. Great care has been taken to obtain homogeneous excitation conditions by focusing the laser spot to a diameter slightly larger than the size of the quantum wire pattern of 100×100 μm^2. In order to avoid any significant sample heating a mechanical chopper has been used that minimizes the average laser power incident on the wires to less than about 0.1 kW cm^{-2}. The emission has been dispersed by a single grating monochromator with a focal length of $f=0.25$ m and detected by a Peltier-cooled $S1$ photomultiplier interfaced with a lock-in amplifier.

B. High-excitation spectra

In order to investigate many-body effects in the neutral quasi-one-dimensional electron-hole plasma, we have performed magneto-photoluminescence studies by using varying optical excitation powers. Figure 2 shows a series of luminescence spectra of 29-nm-wide $In_{0.13}Ga_{0.87}As/GaAs$ quantum wires recorded at $B=10.5$ T. In order to resolve emission features with low intensity more clearly we have plotted the intensities on a logarithmic scale [in Fig. 11(a) the spectra are also shown on a linear intensity scale]. At low excitation one spectral line can be observed with its peak at an energy of $E=1.443$ eV. This emission is due to recombination of quantum-wire ground-state excitons. With increasing excitation power the intensity of the ground-state emission increases continuously and finally it saturates, indicating completely filled ground subbands. Simultaneously an additional spectral line at $E=1.465$ eV can be resolved that arises from transitions between the second lateral subbands, because higher electron and hole subbands are occupied due to Pauli blocking in the ground states. It should be noted that the emission lines do not broaden strongly with increasing excitation, indicating that the plasma temperature increases only slightly. However, due to the finite plasma temperatures that cause a redistribution of carriers from the ground to excited states this excited spectral line can be observed already at rather low excitation intensities at which the emission from the ground state is not yet saturated. The spectral lines are labeled with a pair of subband quantum numbers, namely, the quantum-well subband number $n_z=1$ and the quantum wire subband number $n_x=1,2,3,\ldots$.

Both lines, $1,1_{e\text{-}h}$ and $1,2_{e\text{-}h}$ are seen to shift towards lower energies with increasing excitation power. Figure 3 shows the peak energies of the two features versus the excitation power densities. The second peak $n_x=2$ shifts significantly more strongly to lower energies than the peak of the lowest emission line with $n_x=1$. The energy of the ground-state transition is almost constant up to excitation powers of about 2 kW cm^{-2}, which correspond to situations in which the ground-state emission clearly dominates the spectrum. Only at the highest excitation powers used in the present experiments is a decrease of its position in energy found, which amounts to up to 1.5 meV. In contrast, the higher transition shifts continuously to lower energies by about 5 meV over the whole range of plasma densities.

To investigate the excitation density dependence of the quantum wires further, we have also performed experiments at $B=8.5$ T. The corresponding set of spectra recorded by using varying optical excitation power is shown in Fig. 4 (logarithmic intensity scale) and Fig. 13(a) (linear intensity

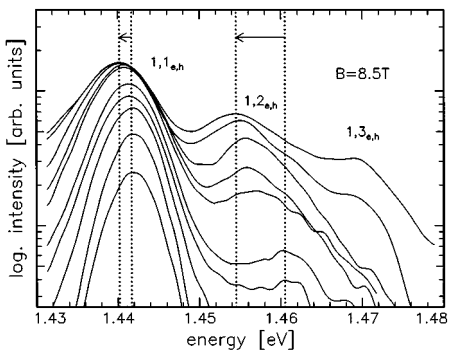

FIG. 4. Luminescence spectra of the 29-nm-wide modulated barrier $In_{0.13}Ga_{0.87}As/GaAs$ wires for various excitation intensities as in Fig. 2, but at $B=8.5$ T.

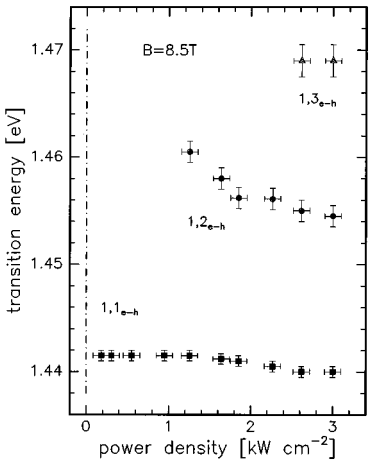

FIG. 5. Transition energies at $B=8.5$ T observed for the 29-nm-wide $In_{0.13}Ga_{0.87}As/GaAs$ quantum wires as functions of the laser power densities.

scale). Due to the decreased intersubband splittings at the lower magnetic field three spectral features can now be resolved at high excitation powers. These features can be attributed to the three electron quantum-wire subbands $n_x=1,2,3$, which are confined in the investigated structures. Similarly to the case of $B=10.5$ T, also here a saturation of the emission intensity from the lower subbands is observed with increasing excitation power in connection with the appearance of higher-lying transitions. Simultaneously the spectral lines shift towards lower energies in qualitatively the same manner as at $B=10.5$ T. Due to the finite temperature of the carriers emission from the higher confined subbands can be already observed when the emission from lower-lying subbands is not yet saturated.

Figure 5 displays the peak energies versus excitation power density of the three spectral lines at $B=8.5$ T. The splitting between the transitions is almost equidistant for the highest excitation powers, at which the splitting between the two lowest lines is 15 meV, whereas the splitting between the two higher lines is with 14 meV slightly smaller. Similarly to the case of $B=10.5$ T the total shift of the second line to lower energies with increasing excitation power is significantly stronger than the low-energy shift of the ground-state emission. The energy of the $1,1_{e\text{-}h}$ emission line decreases only when the higher-lying states are significantly occupied with carriers. On the other hand, the second spectral line does not shift continuously to lower energies. Its energy is almost constant between $\sim$1.9 and 2.2 kW cm^{-2}, which corresponds to situations in which the emission from the ground state is already saturated, but emission from the third quantum wire subbands is not yet observed; i.e., the states $1,3_e$ and $1,3_h$ are not significantly occupied with carriers. However, if the third lateral electron and hole subbands are occupied with carriers, the energy of the first excited transition is again shifted towards lower energies.

In order to analyze these experimental results in detail, a theoretical model is required. As discussed above, the energy scales, which determine the properties of the quasi-one-dimensional system, the cyclotron energy, the exciton binding energy, and the lateral confinement potential are of the same order of magnitude. This leads immediately to the necessity of a theoretical description in which all the effects are treated on the same level.

III. THEORY

A. Assumptions and basic results

In our theoretical model we treat a quantum wire that is embedded in a quasi-two-dimensional (ideal) quantum well by means of some additional lateral confinement. Furthermore, we assume that this lateral confinement potential is smooth and can be modeled by a Gaussian potential, which can be approximated for the lower-lying states by a harmonic oscillator potential. The confinement potential of the modulated barrier quantum wires is actually in between a finite square-well potential and a Gaussian one, but the lowest eigenfunctions in these potentials are at least qualitatively very similar. We make use of the effective-mass approximation, but we neglect band mixing effects because they are expected to be of minor importance for the thin strained nanostructures investigated here.[18] Therefore, we take into account only quantum-wire states that are formed out of the lowest quantum-well electron and heavy-hole subbands, respectively. The single-particle Hamiltonian for an electron ($j=e$) or a hole ($j=h$) moving in the x-y plane with the wire axis in the y direction reads (setting $\hbar=1$)

$$H_j^0=\frac{1}{2m_j}\left(\mathbf{p}_j-\frac{e_j}{c}\mathbf{A}(\mathbf{r}_j)\right)^2+\frac{1}{2}m_j\Omega_j^2x_j^2+\frac{E_g}{2}. \qquad (1)$$

The kinetic energy is modified by the vector potential $\mathbf{A}(r_j)$. The second term is the lateral parabolic confinement potential and characterized by the intersubband frequencies Ω_j . E_g denotes the band gap of the underlying quantum well. The coupling of B to the magnetic moment of the spin (i.e., the Zeeman spin splitting) is neglected here because this term becomes important only for very large magnetic fields.[19] For a magnetic field normal to the quantum well, i.e., in the z direction, the vector potential can be chosen parallel to the wire axis by using the Landau gauge, i.e., $\mathbf{A}(r_j)=x_jB\mathbf{e}_2$, where $\mathbf{e}_2$ is the unit vector in the y direction. The Hamiltonian can easily be diagonalized and one obtains the following eigenfunctions $\psi_{k\ell}^j$ and eigenvalues $\epsilon_{k\ell}^j$:

$$\psi_{k\ell}^j(x,y)=\frac{1}{\sqrt{L_y}}e^{iky}\phi_\ell(x-k\delta_j),\qquad \delta_j=\frac{1}{m_j}\frac{\omega_c^j}{(\omega_c^j)^2+\Omega_j^2}, \qquad (2)$$

$$\epsilon_{k\ell}^j=\frac{\Omega_j^2}{\Omega_j^2+(\omega_c^j)^2}\frac{k^2}{2m_j}+\sqrt{\Omega_j^2+(\omega_c^j)^2}\left(\ell+\frac{1}{2}\right),$$

$$\ell=0,1,\ldots, \qquad (3)$$

where the ϕ_ℓ are normalized harmonic oscillator wave functions, k is the wave number in the wire direction, and $\omega_c^j=e_jB/m_j$ are the individual ($j=e,h$) cyclotron frequencies. $k\delta_j$ is the center of the lateral wave function. The electron and hole wave functions are time-reversal counterparts of each other, respectively:

$$\psi^e_{kl}(x,y)=[\psi^h_{-kl}(x,y)]^\star.$$

As can be seen from Eq. (3), the magnetic field increases the lateral subband spacing as well as the effective mass in wire direction,[20] which is a consequence of the stronger localization of the carriers by the magnetic field. Therefore the magnetic field suppresses the motion along the wire. Two magnetic field regimes can be distinguished: In the low-field regime ($\Omega \gg \omega_c$) the lateral wire width ℓ_x is the characteristic length that determines the quantization of the carriers. In contrast, at high fields ($\Omega \ll \omega_c$) the quantization is determined by the magnetic length $\ell_m=(c/eB)^{1/2}$. The changeover between these two field regimes takes place, when both length scales become comparable.

The magnetic field also shifts the lateral wave functions proportional to the wave number k perpendicular to the wire direction [see Eq. (2)]. At low magnetic fields, the shift is approximately proportional to B. This linear shift with B is a result of the Lorentz force, which is proportional to the velocity of the particle and also proportional to the magnetic field. At high fields, however, the shift is reduced by the field-induced localization so that the carriers are driven back to the center of the wire.

For simplicity, we assume an electron-hole symmetry $m_e\Omega_e=m_h\Omega_h=m\Omega$, where m is the reduced electron-hole mass and Ω the total intersubband spacing. This approximation leads to a local charge neutrality. While the values of k are unrestricted for $B=0$ (besides the restrictions arising from periodic boundary conditions), they are restricted for $B\neq 0$ by the condition that the center of the carrier wave function $k\delta_j$ must lie inside of the quantum wire, which resembles a boundary condition for the assumed harmonic confinement potential:

$$|k\delta_j| \leqslant \frac{L}{2}. \tag{4}$$

By fitting the lateral subband splitting Ω with the energy splitting between the two lowest subbands of a rectangular square well,

$$\Omega=\frac{3\pi^2}{2mL^2}, \tag{5}$$

the following largest allowed wave number $k_{\rm ext}$ is obtained:

$$|a_0 k_{\rm ext}|=\frac{\pi}{4}\sqrt{3\frac{E_0}{\Omega}\left(\frac{\omega_c^2+\Omega^2}{E_0\omega_c}\right)}, \tag{6}$$

where E_0 is the three-dimensional exciton Rydberg and a_0 is the corresponding Bohr radius. Now the density of states $D(E)=\mathrm{Tr}\delta(E-H)$ can be calculated with $k_{\rm min}=-k_{\rm ext}$ and $k_{\rm max}=+k_{\rm ext}$ being the minimum and the maximum allowed values for the wave number k:

$$D(E)=\sqrt{\frac{m}{2\pi^2}}\sum_{\ell}\frac{1}{\sqrt{E-\sqrt{\Omega^2+\omega_c^2}\left(\ell+\frac{1}{2}\right)}} \times[\Theta(k_{\rm max}-k(E))+\Theta(k(E)-k_{\rm min}))], \tag{7}$$

with $k(E)=\sqrt{2m[(\Omega^2+\omega_c^2)/\Omega^2](E-E_\ell)}$.

With increasing magnetic field the single-particle density of states changes from the $1/\sqrt{E}$-like behavior of a 1D system to the δ-function-like behavior of a totally confined system. Calculating now the total number of states g in a quasi-one-dimensional subband with index ℓ, one finds the relation

$$g\propto\sqrt{\frac{\Omega^2+\omega_c^2}{\Omega^2}}. \tag{8}$$

In contrast to a quantum well in normal magnetic fields, for which the number of states on a Landau level depends only on the magnetic field and increases linearly with B, the number of states in a quantum wire subband is almost constant in the low-field regime. Only in the high-field regime does g increase linearly with B.

Because the electrons and holes are charged particles, one has to take into account their mutual Coulomb forces. If the field lines between two particles can also penetrate into the barrier material arround the quantum wire, one obtains for the quasi-one-dimensional Coulomb interaction matrix elements $V^{jj'}_{\ell\ell'}(q)$ as functions of the transferred momentum in wave-number space

$$V^{jj'}_{\ell\ell'}(q)=\sum_{q'}\frac{2\pi e_j e_{j'}}{\epsilon_0\sqrt{q^2+q'^2}}\left|\int dx\,\phi^*_\ell(x+\delta q)e^{ixq}\phi_{\ell'}(x)\right|^2, \tag{9}$$

where ϵ_0 is the static dielectric constant of the quantum wire material. The total (difference) momentum in the e-e, h-h, and e-h channels is taken to be zero. For $j=j'$ Eq. (9) defines the electron-electron and hole-hole exchange Coulomb interactions, which determine the subband renormalization. Simultaneously, Eq. (9) defines the direct e-h Coulomb interaction, which is relevant for excitonic effects. These Coulomb matrix elements can be understood as an averaged bare two-dimensional interaction with respect to the lateral single-particle wave functions.

For a parabolic confinement potential the eigenfunctions [see Eq. (2)] are known explicitly so that the Coulomb matrix elements can be calculated analytically and are given in the Appendix. To our knowledge, explicit results for the one-dimensional Coulomb matrix elements for several subbands have only been published without a magnetic field.[21]

It is seen that the Coulomb matrix elements depend only in a parametric way on the ratio of the cyclotron frequency ω_c to an effective total intersubband spacing $\Omega^*=\sqrt{\omega_c^2+\Omega^2}$ and on the dimensionless wave number qa_c where $a_c=1/(m\Omega^*)^{1/2}$ is the amplitude of the zero-point motion. In Figs. 6 and 7 we show numerical results for the wave-number dependence of the Coulomb matrix elements for several subband indices in the two limiting cases $\omega_c/\Omega^*=0$ and 1, respectively, i.e., without a magnetic field and for magnetic fields, where the magnetic confinement clearly dominates the geometric one ($B\to\infty$). Only the matrix elements describing the e-e or the h-h interactions are shown. Without a magnetic field the diagonal matrix elements are always larger than the off-diagonal elements. A magnetic field causes large changes of the matrix elements. Due to the shifted single-particle wave functions for large values of qa_c, the off-diagonal elements become larger than

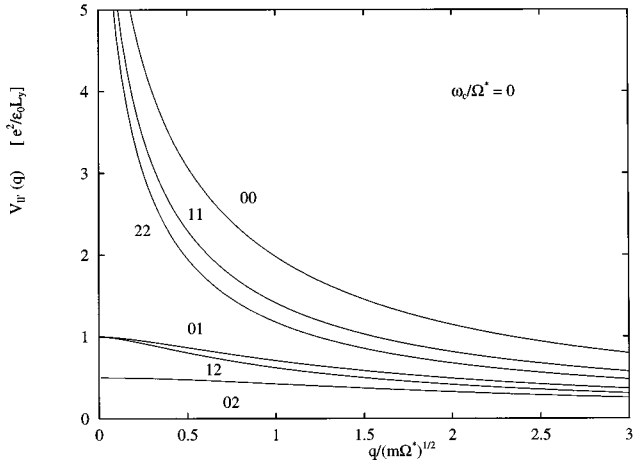

FIG. 6. Intraband and interband Coulomb matrix elements ($j=j'$, i.e., describing the e-e or the h-h interaction) as functions of the wave number q at zero magnetic field ($\omega_c=0$); the numbers indicate the lateral subband quantum numbers.

the diagonal ones. For small wave numbers ($q\to 0$) the diagonal elements with and without a magnetic field diverge logarithmically, whereas the off-diagonal elements remain finite in both cases. The matrix elements at finite magnetic fields do not decrease monotonically because of the k-dependent shift of the electron and hole wave functions. Therefore the maxima and the minima of these wave functions are at different positions for different k values, resulting in a quasioscillating behavior of the wave-function overlap.

B. Magneto-optical spectra

The magneto-optical spectra are calculated for a laser excited electron-hole plasma that has relaxed into a quasiequilibrium state. Although relaxation and carrier capture processes may be significantly slowed down in quasi-one-dimensional structures,[22–25] we assume that the relaxation process is completed within the carrier lifetime. In this situation the occupation numbers of the individual subbands

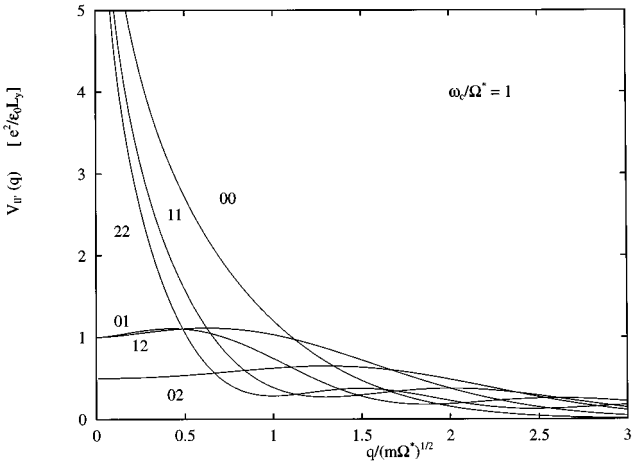

FIG. 7. Coulomb matrix elements as functions of the wave number q as in Fig. 6, but at a very strong magnetic field, so that the lateral confinement is negligible.

states are described by Fermi distributions $f_{k\ell}$ with one chemical potential for the electrons and the holes, respectively. The coupling between the electron-hole system and the external light field is described within the dipole approximation. If we neglect the (small) photon momentum, the light field (in our model) couples only subband states with equal quantum numbers.

As discussed in the Introduction we calculated all many-body effects within the Hartree-Fock approximation, because screening in one-dimensional structures is a relatively small effect compared to band filling, excitonic correlations, and the strong influence of the magnetic field. We stress again that the use of an unscreened Coulomb potential in the calculations of the self-energies and of the interband density matrix elements forms a conserving approximation, which fulfills Ward identities.[11] We calculate the optical susceptibility within the so-called ladder approximation. The interband matrix element of the single-particle reduced density matrix obeys an integral equation in which the attractive electron-hole Coulomb interaction determines the integral kernel.[11] This equation can be transformed into an integral equation for the optical susceptibility components $\chi_{k\ell}$ (the interband matrix element d_{cv} is assumed to be a constant)

$$\chi_{k\ell}(\omega)=\chi^0_{k\ell}(\omega)-\chi^0_{k\ell}(\omega)\frac{1}{d_{cv}}\sum_{k',\ell'} V^{eh}_{\ell\ell'}(k-k')\chi_{k'\ell'}(\omega), \tag{10}$$

where the free-particle susceptibility $\chi^0_{k\ell}(\omega)$ in the spectral representation[26] is given by

$$\begin{aligned}\chi^0_{k\ell}(\omega)&=d_{cv}\int_{-\infty}^{\infty}\frac{d\omega'}{\pi}\frac{\gamma}{(\omega'-\epsilon^e_{k\ell}-\epsilon^h_{k\ell})^2+\gamma^2}\\&\quad\times\frac{[1-f(\omega'-\epsilon^e_{k\ell})-f(\epsilon^h_{k\ell})]}{\omega'-\omega-i\delta}\\&\simeq d_{cv}\frac{\epsilon^e_{k\ell}+\epsilon^h_{k\ell}-\omega}{(\epsilon^h_{k\ell}+\epsilon^e_{k\ell}-\omega)^2+\gamma^2}[1-f(\epsilon^e_{k\ell})-f(\epsilon^h_{k\ell})]\\&\quad-id_{cv}\frac{\gamma}{(\epsilon^e_{k\ell}-\epsilon^h_{k\ell}-\omega)^2+\gamma^2}\\&\quad\times[1-f(\omega-\epsilon^h_{k\ell})-f(\epsilon^h_{k\ell})].\end{aligned} \tag{11}$$

Here, $\epsilon^j_{k\ell}$ are the single-particle energies [see Eq. (3)] renormalized by the exchange energy, that is,

$$\epsilon^j_{k\ell}\to\epsilon^j_{k\ell}-\sum_{k',\ell'} V^{jj}_{\ell\ell'}(k-k')f(\epsilon^j_{k'\ell'}). \tag{12}$$

The Lorentzian spectral functions are characterized by a single broadening constant γ. $f(\epsilon^i_{k\ell})$ are the thermal Fermi distribution functions for the electrons and the holes, respectively. The total susceptibility is obtained by summing over all wave numbers k and all subbands ℓ:

$$\chi(\omega)=\sum_{k,\ell} d^*_{cv}\chi_{k\ell}(\omega). \tag{13}$$

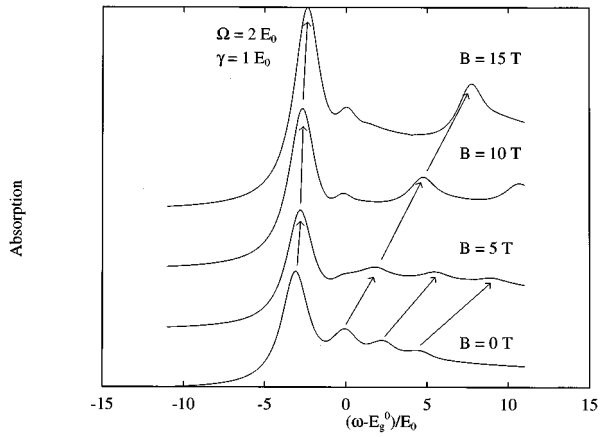

FIG. 8. Absorption spectra of an $In_{0.13}Ga_{0.87}As/GaAs$ quantum wire for varying magnetic fields. The lateral subband spacing Ω is two times the excitonic Rydberg E_0 and the broadening is assumed to be one Rydberg.

The absorption coefficient $\alpha(\omega)$ is given by the imaginary part of the optical susceptibility, $\alpha(\omega)=\mathrm{Im}\chi(\omega)$. The real part of $\chi(\omega)$ determines the reflectivity $r(\omega)$. For the calculation of the optical spectra one has to solve a set of (linear) coupled integral equations by a numerical matrix inversion procedure.[26,27]

In a quantum well the magnetoexciton spectrum consists of bound states. Only the excitons with magnetic quantum number $m=0$ (s states) are optically active; that is, in each Landau level only one exciton state is optically active. This magnetic quantum number is no longer a good quantum number in quantum wires because the lateral confinement breaks the in-plane rotational symmetry. As discussed above, the carriers can move along the wire also when a normal magnetic field is applied to the structure. Consequently the exciton spectrum of a quantum wire is hydrogenlike, i.e., it consists of both an infinite number of bound states and a continuum of scattering states.[28,29] The restriction of the k space by Eq. (4) restricts also the number of bound states to a finite number.

Figure 8 shows absorption spectra of a quantum-well wire made of $In_{0.13}Ga_{0.87}As/GaAs$ with a subband spacing $\Omega=2E_0\simeq 8.4$ meV (E_0 is the three-dimensional exciton Rydberg of GaAs) for zero plasma density. The spectra are shifted vertically to each other for increasing magnetic fields. The frequency ω is measured from the one-dimensional band edge E_g^0 in units of E_0. The spectrum for $B=0$ shows four excitonic resonances that belong to the ground-state excitons of the lowest four one-dimensional subbands. It is seen that the lowest exciton state (i.e., the one from the lowest subband) has the largest oscillator strength. By applying a magnetic field the absorption spectrum changes in various aspects. First, for finite magnetic fields all spectra are blueshifted. This indicates that the localization energy due to the magnetic field is always larger than the increased electron-hole binding energy due to the modified quasi-one-dimensional Coulomb interaction. The blueshift of the ground state is considerably smaller than the shift of the higher states, indicating the bound nature of the ground state; i.e., the binding energy of the ground-state exciton is significantly more strongly increased with increasing B than that of the excited excitons.

For low magnetic fields (when the cyclotron frequency is smaller than the subband spacing) the shift of the ground state exciton is diamagnetic proportional to B^2. In addition, the oscillator strength of the ground-state exciton is to a good approximation constant in this field regime. For large magnetic fields (where the cylotron frequency is larger than the subband spacing) we obtain in contrast a clearly increasing oscillator strength for increasing magnetic fields. In this regime the influence of the lateral confinement potential becomes small and the main features in the optical spectra resemble the features in the spectra of a quantum well in a normal magnetic field.[30,31] We obtain resonances with large oscillator strengths in the absorption spectrum, which correspond to the Landau levels with their energies given in terms of the combined (electron and hole) cyclotron frequency.

As stated above, the exciton spectrum of a quantum wire consists of bound states and scattering states. Consequently not only the ground-state excitons can be observed in the absorption spectra for magnetic fields $\geqslant 5$ T, but also weak additional features appear with energies between those of the ground-state excitons of the lowest and the first excited lateral subbands. These features correspond to the lowest excited bound exciton states of the lowest subbands. At 10 T only one excited bound state is observed; at 15 T indications for a second excited state can be found. Moreover, it should be noted again that no indications for the $1/\sqrt{E}$ singularity can be found at the onset of the continuum of scattering states. The disappearance of this divergency originates from the strong redistribution of oscillator strength to the ground-state exciton, which is a consequence of the excitonic correlations. These correlations cause the ''Sommerfeld factor'' to be smaller than unity in contrast to most systems of higher dimensionality.

Luminescence spectra can be calculated by using the relation

$$I(\omega)\sim\frac{\mathrm{Im}\chi(\omega)}{e^{\beta(\omega-\mu)}-1}, \tag{14}$$

where μ is the combined (electron and hole) chemical potential. An example for a spectrum of a highly excited $In_{0.13}Ga_{0.87}As$ quantum wire is shown in Fig. 9 for different magnetic fields. Again, the origin of the frequency is the unrenormalized subband edge and is measured in excitonic units of E_0. The spectra for several values of B are again shifted vertically to each other. For the assumed plasma density of $na_0=4$ all four subbands are populated at $B=0$. Because the broadening is chosen to be smaller than the subband spacing, we obtain for low magnetic fields four distinct peaks that are connected with the corresponding subband edges. In the high-field limit the spectrum is described to a good approximation by Landau levels separated by the sum of the electron and hole cyclotron frequencies and it approaches that of a quantum well in a normal magnetic field.[30,31]

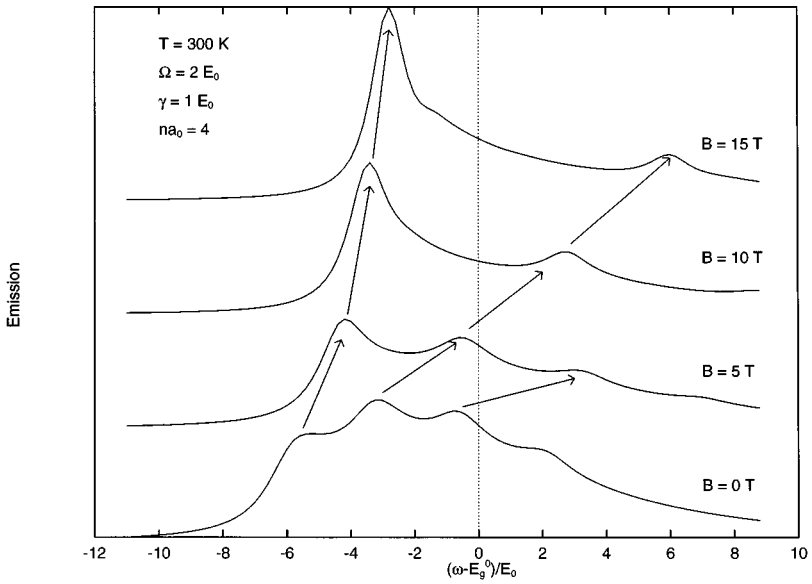

FIG. 9. Calculated luminescence spectra of a highly excited $In_{0.13}Ga_{0.87}As/GaAs$ quantum wire at varying magnetic field strengths. The plasma temperature is 300 K and the plasma density is $na_0=4$. The rest of the parameters are identical to those chosen for the calculation of the absorption spectra.

IV. COMPARISON OF EXPERIMENTAL AND THEORETICAL SPECTRA

The quantum-wire structures that were investigated in the present experiments meet the restrictions imposed by the basic theoretical assumptions quite well. In detail, the wires are embedded in a two-dimensional quantum well, as shown schematically in the inset of Fig. 1. The lateral confining potential in the modulated barrier wires is close to a rectangular shape. Nevertheless, its shallowness creates subband spacings which are approximately equidistant. The difference in energy between the second and the first excited lateral subbands is even slightly smaller than the difference between the first and the ground subbands for the investigated wires. Furthermore, in Ref. 7 we modeled the single-particle states in these quantum wires subject to magnetic fields by assuming rectangular geometric confinement potentials. We calculated both the single-particle eigenstates and eigenfrequencies. While the wave functions show some deviations from parabolic ones, particularly at the semiconductor/vacuum interface, the energies as functions of the magnetic field differ only slightly from those calculated in the parabolic approximation. This indicates that in the present quantum wires the matrix elements are not very sensitive to the particular shape of the confining potential.

The strain due to the lattice mismatch between $In_{0.13}Ga_{0.87}As$ and GaAs causes a splitting of the heavy-hole and light-hole subband edges of about 60 meV, which is larger than the lateral confinement potential. Therefore the influence of band mixing will be small and the highest quantum well valence subband has a heavy-hole character and can be described by a simple parabolic band.

In studies using a sufficiently intense optical excitation in order to observe emission from higher lateral subbands, the transformation of the electron hole plasma from quasi-one- to quasi-zero-dimensionality with increasing magnetic field has already been shown earlier.[7] In the wires investigated here the lateral subband splitting amounts to about $\Omega=10$ meV. This splitting requires magnetic fields of about $B=5$ T for the 1D-0D transition. The transition is accompanied by a strong exchange of oscillator strength between the observed lateral subband transitions.

Under high excitation the emission intensity from the lowest subbands is saturated for all applied magnetic fields. Figure 10 shows the integrated luminescence intensity of the ground-state transition normalized by its integrated intensity at $B=0$. For small magnetic fields the intensity remains almost constant up to $B=5$ T, where the transition to completely quantized behavior occurs. Above 5 T the intensity of the lowest subband transition increases almost linearly with B. The equivalent behavior has already been observed in the calculated luminescence spectra in Fig. 10. Assuming that the first subband is in all cases completely occupied at an approximately constant plasma temperature, the integrated luminescence intensity is proportional to the total number of states g in a subband. It thus reflects the one-dimensional behavior of g in a quantum wire subband as given by Eq. (7).

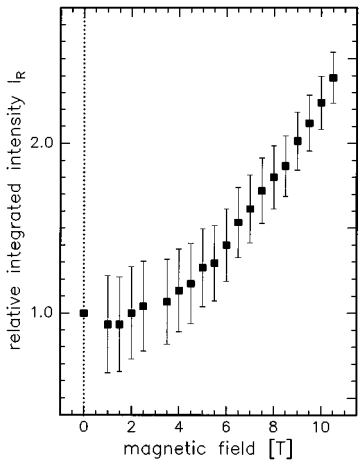

FIG. 10. Integrated luminescence intensity of the ground-state transition of 29-nm-wide $In_{0.13}Ga_{0.87}As/GaAs$ quantum wires as a function of the magnetic field. The intensities have been determined from high excitation spectra (excitation powers >2 kW cm^{-2}) so that the electron and hole ground states were completely filled with carriers, i.e., the ground-state emission is saturated.

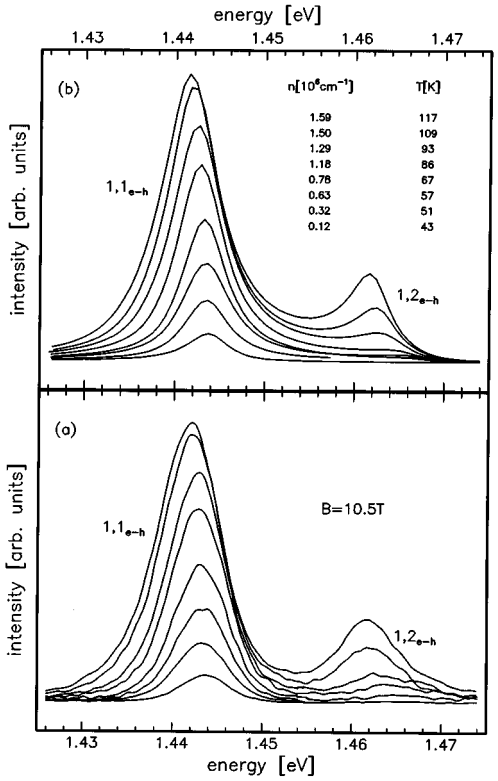

FIG. 11. (b) Calculated line shapes for the modulated barrier $In_{0.13}Ga_{0.87}As/GaAs$ quantum wires at $B=10.5$ T in order to fit the experimentally recorded luminescence spectra, which are displayed in (a). The plasma densities and the plasma temperatures that have been determined from the line shape analysis are shown in (b).

The number of states in one subband increases with increasing magnetic field, leading to a depopulation of higher subbands. Simultaneously the subband spacing is increased so that the oscillator strengths of the lower transitions are enhanced and the lowest resonance dominates at high magnetic fields. As observed experimentally, this increase shows a highly nonlinear dependence on B in quantum wires, in contrast to the emission intensity from a Landau level in a quantum well that increases linearly with B.

Next we study many-body effects in the dense neutral quasi-one-dimensional magnetoplasma at $B=10.5$ T. For that reason we have fitted the measured spectra with our calculations by adjusting the temperature and the density of the carriers only, while for the rest of the parameters experimentally determined values have been used.[32] As can be seen from the comparison of the experimental spectra in Fig. 11(a) and the calculated spectra in Fig. 11(b), excellent agreement is obtained with respect to both the line shape and the oscillator strength of the observed transitions. Particularly, the saturation of the lowest emission line $1,1_{e\text{-}h}$ and the simultaneous increase of the second emission line $1,2_{e\text{-}h}$ is described quite well within our model. Here we want to emphasize again that the excellent agreement of the line shapes is only obtained if the momentum cutoff discussed in Sec. III A is used in the calculations.[33]

From the lineshape analysis we obtain plasma densities that increase from about 0.1×10^6 cm^{-1} at the lowest excitation up to about 1.6×10^6 cm^{-1} at the highest excitation. Simultaneously the plasma temperatures increase only slightly, but continuously from about 40 K to about 120 K.[34] This moderate increase clearly indicates that sample heating effects can be excluded. The plasma densities and the plasma temperatures that were determined from the line-shape analysis are displayed in Fig. 11(b) for the set of luminescence spectra at $B=10.5$ T.

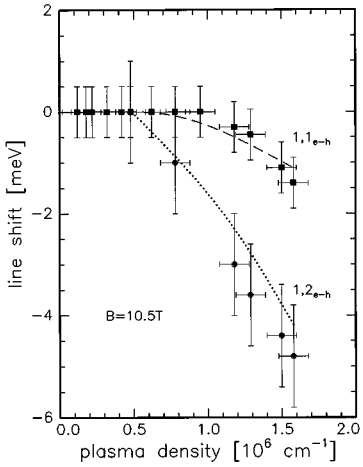

FIG. 12. Shift of the emission lines to lower energies for the modulated barrier $In_{0.13}Ga_{0.87}As/GaAs$ quantum wires as a function of the total plasma density at $B=10.5$ T. The symbols show the experimental data, while the lines show the results of the calculations.

The position in energy of the lowest subband emission does not change with increasing plasma density until the second subband begins to be significantly occupied. Naturally the absence of a peak shift should not be taken as a sign of the absence of a band-gap shift. In this regime the band-gap shifts and the excitonic correlations compensate each other completely. Figure 12 shows the shift of the ground-state transition (squares) and of the first excited transition (circles) as a function of the total plasma density (i.e., the plasma density in both occupied subbands) for a magnetic field of 10.5 T. At densities below about 0.6×10^6 cm^{-1} only the lowest subband is occupied and the density dependence of the band-gap renormalization and of the excitonic correlations cancel completely. At densities above 0.6×10^6 cm^{-1} both transitions shift towards lower energies due to the dominance of the band-gap renormalization over the excitonic correlations. At the highest plasma densities this shift is 1.5 meV for the ground-state transition and it amounts to about 5 meV for the first excited level. As indicated by the dashed (ground state) and dotted lines (first excited state), the calculated shifts are in good agreement with the experiments.

The observed low-density behavior is very well known for excitons in one Landau level, where an exact cancellation occurs due to the inherent symmetry of the two-dimensional neutral carrier system, which makes the e-e and h-h interactions equal to the e-h interactions.[35–44] Therefore the quasi-two-dimensional electron-hole system in one Landau level forms an ideal gas. However, this cancellation does not hold for excitons from different Landau levels: Whereas the exchange interaction remains significant, the Pauli repulsion responsible for the exciton-exciton interaction is significantly reduced. The renormalization of one subband is therefore

determined by the occupation of the other subbands. This behavior is completely different from the behavior of a quasi-one-dimensional plasma at zero magnetic field, where the renormalization is determined mainly by the occupation of the subband itself, whereas interband contributions are comparatively small.[10]

In Ref. 45 general conditions have been formulated for the formation of a singlet quantum state of noninteracting composite particles (ideal gas). These conditions are as follows: (i) the system contains two kinds of particles for which the matrix elements describing the (arbitrary) interparticle interaction are symmetric. (ii) The spectra of the free particles in the two-component system are degenerate with each other. Both conditions are not exactly, but to a good approximation, fulfilled for quantum wires subject to high magnetic fields: as was shown in Ref. 45 the possibility of such an exact solution for a many-body system arises from its symmetry under continuous rotations in the isospin space of the two components of particles that form the quantum system. While without magnetic field this symmetry is broken in both quantum wells and wires, it is exactly fulfilled for a two-dimensional electron-hole system in magnetic field. For quantum wires the lateral confinement potential breaks the symmetry, because also in a magnetic field motion of the free carriers along the wire is possible and therefore the single-particle spectra are not degenerate. However, as was discussed already in Sec III, this carrier motion is continuously suppressed by B. In the high-field regime, in which the magnetic length is clearly smaller than the wire width, the dispersion along the wire becomes small and the isospin symmetry is then to a good approximation restored.

Due to the finite carrier temperatures emission from the second subband can be observed already at rather small plasma densities, at which the lowest subband is not completely filled. With increasing plasma densities the second subband peak is shifted strongly towards lower energies, as expected from the strong population of the lowest subband. If one compares this renormalization with that in a quasi-two-dimensional magnetoplasma system over equivalent plasma densities, the low-energy shift is enhanced in the quantum wire by about 50%. This can be understood qualitatively in the following way: in the case of a two-dimensional system it is well known that the magnetic-field-induced localization enhances the interparticle interaction and therefore the renormalization.[39] In the present high-magnetic-field studies we work in a regime where the magnetic confinement dominates the lateral confinement potential. This situation equals that of a two-dimensional system in an accordingly higher magnetic field. This effectively higher magnetic field explains the enhanced renormalization.

We have analyzed also the experiments performed at $B=8.5$ T. At this field strength the carriers are still in the high-field, quasi-zero-dimensional regime, but the splitting between the subbands is significantly reduced by about 4–5 meV. As shown in Fig. 13(b), this allows us to populate even three lateral subbands. In the present structures the subband spacing between the third and the second subbands is slightly smaller than that between the second and first subbands, while in our harmonic oscillator model the subbands are equidistantly spaced. Because of the larger spacing in energy we are not able in our calculations [see Fig. 13(b)] to populate the third lateral subband as strongly as it is populated in the experiments [Fig. 13(a)]. Here we find that the plasma density is continuously increased from about 0.1×10^6 cm^{-1} to about 2×10^6 cm^{-1} with increasing excitation, while the plasma temperatures increase moderately from about 40 K to about 140 K.

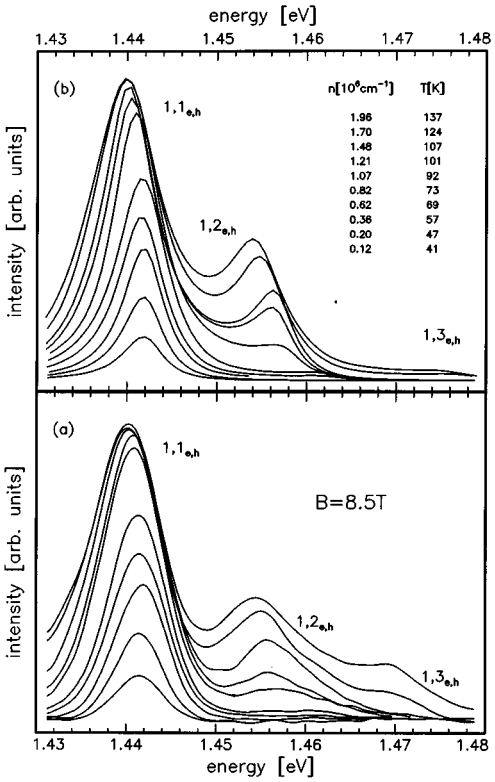

FIG. 13. (b) Calculated luminescence spectra at $B=8.5$ T for the modulated barrier $In_{0.13}Ga_{0.87}As/GaAs$ quantum wires in comparison with the experimental spectra (a). The plasma densities and plasma temperatures are displayed in (b).

Nevertheless, the principal features of both the experimental and the theoretical spectra agree very well and the observed behavior is very similar to that observed at $B=10.5$ T. The lowest subband emission saturates with increasing excitation power and emission from higher lateral subbands is observed. The lowest subband emission is only shifted to lower energies when the higher subbands are populated. In addition, also the peak of the second subband line does not shift, when the lowest electron and hole subbands are completely filled and in addition the third subband is not yet populated strongly, as can be seen in the third and fourth spectra from the top in Fig. 13(a).

Figure 14 shows the shift of the luminescence lines of the ground-state transition (experimental data by squares) and of the first excited state (experimental data by circles) in comparison with the results of the calculations (dashed and dotted lines, respectively). As can be seen from both the experimental and theoretical results first there is no resolvable shift of the ground-state transition at low plasma densities smaller than about 0.8×10^6 cm^{-1}, at which higher states are not populated. Second, when the first excited electron and hole subbands are populated we observe a redshift of the ground-state transition energy and also of the transition energy of the

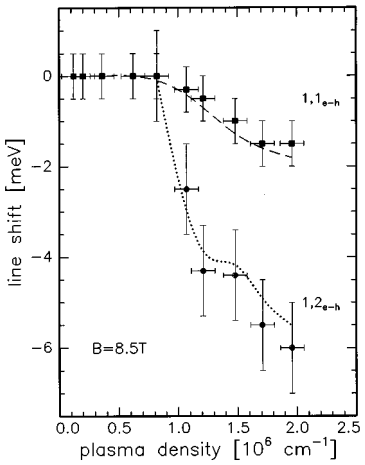

FIG. 14. Shift of the spectral lines for the modulated barrier $In_{0.13}Ga_{0.87}As/GaAs$ quantum wires as a function of the total plasma density at $B=8.5$ T. Squares and circles, experimental data; dashed and dotted lines, calculated lines for the ground- and first-excited-state transitions, respectively.

first excited state, until the ground subbands are completely filled with carriers. Third, at plasma densities in excess of 1.5×10^6 cm^{-1} a further shift of the first excited-state transition energy is observed, which can be assigned, by comparison with the calculations, to the interaction between carriers in the first and second excited levels. This confirms that the renormalization of one subband in the neutral magnetoplasma in quantum wires is mainly determined by the occupation of the other subbands, whereas the contributions from carriers within the subband are comparatively small.

V. SUMMARY

We have calculated magneto-optical absorption and luminescence spectra of optically excited quantum well wires. The luminescence spectra show a transition from quasi-one-dimensional behavior at low magnetic fields (where one has a strong mixing of lateral and magnetic confinement) to quasi-zero-dimensional behavior at high magnetic fields. The calculations make use of a parabolic wire confinement potential in which the single-particle states in an arbitrarily large magnetic field can be calculated exactly. We used a Hartree-Fock approximation and included excitonic effects as well as phase space filling due to an electron-hole plasma and band-gap renormalization consistently.

Luminescence spectra of modulated barrier $In_{0.13}Ga_{0.87}As/GaAs$ quantum wires in magnetic fields up to 10.5 T have been recorded for various excitation intensities. The transition to quasi-zero-dimensional behavior has been confirmed by the magnetic field dependence of the integrated luminescence intensity of the lowest subband emission, which is proportional to the total number of states per subband. Excitation-intensity-dependent luminescence spectra are in excellent agreement with the calculated plasma-density-dependent spectra, provided one takes into account that the electron and hole momenta have to be small enough that the Lorentz force due to the magnetic field does not push the particles out of the wire potential well. Our studies show that the band-gap renormalization of a subband in the dense neutral quasi-one-dimensional magnetoplasma is mainly determined by the population of the other subbands. This is a characteristic difference from studies at $B=0$, which clearly show that the renormalization at zero field is due to carrier-carrier interactions in the same subband.

ACKNOWLEDGMENTS

We would like to thank Professor V. D. Kulakovskii for useful discussions. This work has been supported partially by the Deutsche Forschungsgemeinschaft and the Volkswagen Stiftung.

APPENDIX

In this appendix we give analytical expressions for the quasi-one-dimensional Coulomb interaction matrix elements up to the third subband, which were calculated in a parabolic approximation. Defining an effective intersubband spacing energy $\Omega^*=\sqrt{\omega_c^2+\Omega^2}$ and the variables $x=q^2/4m\Omega^*=(a_cq)^2$ and $y=2x(\omega_c/\Omega^*)^2$, we can express the matrix elements in terms of zeroth-(K_0) and first-order (K_1) modified Bessel functions. We give the matrix elements for the electron-electron and the hole-hole interaction ($j=j'$):

$$V_{00}=\frac{e^2}{\epsilon_0}e^{x-y}K_0(x),$$

$$V_{01}=\frac{e^2}{\epsilon_0}e^{x-y}\{yK_0(x)+x[K_1(x)-K_0(x)]\},$$

$$V_{11}=\frac{e^2}{\epsilon_0}e^{x-y}[1+2x+2x^2+y(y-2x-2)K_0(x)+x(2y-1-2x)K_1(x)],$$

$$V_{02}=\frac{e^2}{\epsilon_0}e^{x-y}\left[\left(x^2-xy+\frac{1}{2}y^2\right)K_0(x)-\left(x^2-\frac{1}{2}x-xy\right)K_1(x)\right], \tag{A1}$$

$$V_{12}=\frac{e^2}{\epsilon_0}e^{x-y}K_1(x)\left[2\left(x^3+\frac{5}{2}x^2+x\right)-y\left(3x^2+\frac{5}{2}x\right)+y^2\frac{3}{2}x\right]-\frac{e^2}{\epsilon_0}e^{x-y}K_0(x)\left[\left(2x^3+\frac{7}{2}x^2+2x\right)-y(3x^2+4x+1)+y^2\left(\frac{3}{2}x+1\right)-y^3\right],$$

$$V_{22}=\frac{e^2}{\epsilon_0}e^{x-y}K_0(x)\left[\left(2x^4+7x^3+\frac{35}{4}x^2+4x+1\right)\right]+\frac{e^2}{\epsilon_0}e^{x-y}K_0(x)\frac{y}{4}[(y^3-4y^2(x+2)+4y(3x^2+6x+5)-(16x^3+44x^2+40x+16)].$$

[1] M. Tsuchiya, J. M. Gaines, R. H. Yan, R. J. Simes, P. O. Holtz, L. A. Coldren, and P. M. Petroff, Phys. Rev. Lett. **62**, 466 (1989).

[2] D. Gershoni, J. S. Weiner, S. N. G. Chu, G. A. Baraff, J. M. Vandenberg, L. N. Pfeiffer, K. West, R. A. Logan, and T. Tanbun-Ek, Phys. Rev. Lett. **65**, 1631 (1990).

[3] Ch. Gréus, L. Butov, F. Daiminger, A. Forchel, P. A. Knipp, and T. L. Reinecke, Phys. Rev. B **47**, 7626 (1993); Ch. Gréus, R. Spiegel, P. A. Knipp, T. L. Reinecke, F. Faller, and A. Forchel, *ibid.* **49**, 5753 (1994).

[4] P. Ils, A. Forchel, K. H. Wang, Ph. Pagnod-Rossiaux, and L. Goldstein, Phys. Rev. B **50**, 11 746 (1994).

[5] M. Kohl, D. Heitmann, P. Grambow, and K. Ploog, Phys. Rev. Lett. **63**, 2124 (1989).

[6] Y. Nagamune, Y. Arakawa, S. Tsukamoto, M. Nishioka, S. Sasaki, and N. Miura, Phys. Rev. Lett. **69**, 2963 (1992).

[7] M. Bayer, A. Forchel, I. E. Itskevich, T. L. Reinecke, P. A. Knipp, Ch. Gréus, R. Spiegel, and F. Faller, Phys. Rev. B **49**, 14 782 (1994).

[8] M. Oestreich, A. P. Heberle, W. W. Rühle, H. Lage, D. Heitmann, and K. Ploog, J. Lumin. **60/61**, 390 (1994).

[9] S. Benner and H. Haug, Europhys. Lett. **16**, 579 (1991).

[10] K. H. Wang, M. Bayer, A. Forchel, P. Ils, S. Benner, H. Haug, Ph. Pagnod-Rossiaux, and L. Goldstein, Phys. Rev. B **53**, 9678 (1996); Ch. Gréus, A. Forchel, R. Spiegel, F. Faller, S. Benner, and H. Haug, Europhys. Lett. **34**, 213 (1996).

[11] H. Haug and S. W. Koch, *Quantum Theory of the Optical and Electronic Properties of Semiconductors*, 3rd ed. (World Scientific, Singapore, 1994).

[12] R. Cingolani, R. Rinaldi, M. Ferrara, G. C. La Rocca, H. Lage, D. Heitmann, and H. Kalt, Phys. Rev. B **48**, 14 331 (1993).

[13] H. Kalt, J. Lumin. **60/61**, 262 (1994).

[14] M. Grundmann, J. Christen, D. Bimberg, and E. Kapon, *The Physics of Semiconductors*, Proceedings of the 22nd International Conference on the Physics of Semiconductors (World Scientific, Singapore, 1995), Vol. 2, p. 1675.

[15] B. Y. K. Hu and S. Das Sarma, Phys. Rev. Lett. **68**, 1750 (1992).

[16] B. Y. K. Hu, Phys. Rev. B **47**, 1687 (1993).

[17] S. Benner and H. Haug, Phys. Rev. B **47**, 15 750 (1993).

[18] U. Bockelmann and G. Bastard, Phys. Rev. B **45**, 1700 (1992).

[19] *Physics of Group IV Elements and III-V Compounds*, 3rd ed., edited by O. Madelung, M. Schulz, and H. Weiss, Landolt-Börnstein, New Series, Group III, Vol. 17, Pt. a (Springer, Berlin, 1982).

[20] K.-F. Berggren, T. J. Thomson, D. J. Newson, and M. Pepper, Phys. Rev. B **37**, 1769 (1986).

[21] G. V. Hu and R. F. O'Connel, Phys. Rev. B **42**, 1290 (1990).

[22] L. W. Molenkamp and M. J. M. de Jong, Phys. Rev. B **49**, 5038 (1994).

[23] S. Das Sarma and C. B. Campos, Phys. Rev. B **49**, 1867 (1994).

[24] M. Oestreich, W. W. Rühle, D. Heitmann, and K. Ploog, Phys. Rev. Lett. **70**, 1682 (1993).

[25] T. Takagahara, Phys. Rev. Lett. **71**, 3577 (1993).

[26] H. Haug and S. Schmitt-Rink, Prog. Quantum Electron. **9**, 3 (1984).

[27] S. Benner and H. Haug, Z. Phys. B **84**, 81 (1991).

[28] For a discussion of absorption spectra of quantum wires at zero magnetic field see, for example, S. Glutsch and D.S. Chemla, Phys. Rev. B **53**, 15 902 (1996), and references therein.

[29] M. Graf, P. Vogl, and A. B. Dzyubenko, Phys. Rev. B **54**, 17 003 (1996).

[30] Ch. Stafford, S. Schmitt-Rink, and W. Schäfer, Phys. Rev. B **41**, 10 000 (1990).

[31] L. V. Butov, V. D. Kulakovskii, G. E. W. Bauer, A. Forchel, and D. Grützmacher, Phys. Rev. B **46**, 12 765 (1992).

[32] The splitting in energy between the lateral subbands has been taken from the experiments (Ref. 3). The broadening constant γ was chosen to be equal to the luminescence half-width of low excitation spectra, which is 2 meV. In addition, in order to obtain estimates for the carrier temperatures we analyzed the high-energy tails of spectra recorded at $B=0$ for different excitation powers. These values are also in good agreement with the values determined from the line-shape analysis.

[33] Without this cutoff the calculated spectra reproduce the experimental ones badly because the spectral lines at high magnetic fields are not symmetric, but show a strong asymmetry due to a high-energy tail that arises from transitions involving states with large k numbers. These transitions are forbidden by the momentum cutoff.

[34] The plasma temperatures in the present experiments are significantly smaller than those in the experiments reported in Ref. 10. The origin of these different behaviors is not fully understood, but might arise from different relaxation of the carriers in the effectively buried structures, which might in addition be altered by the magnetic field.

[35] J. B. Stark, W. H. Knox, and D. S. Chemla, Phys. Rev. Lett. **65**, 333 (1990).

[36] L. V. Butov, V. D. Kulakovskii, and E. I. Rashba, Pis'ma Zh. Eksp. Teor. Fiz. **53**, 104 (1991) [JETP Lett. **53**, 109 (1991)].

[37] L. V. Butov and V. D. Kulakovskii, Pis'ma Zh. Eksp. Teor. Fiz. **53**, 444 (1991) [JETP Lett. **53**, 466 (1991)].

[38] V. D. Kulakovskii and L. V. Butov, Phys. Status Solidi B **173**, 345 (1992).

[39] M. Bayer, A. Dremin, F. Faller, A. Forchel, V. D. Kulakovskii, B.

N. Shepel, and T. Andersson, Phys. Rev. B **50**, 17 085 (1994).
[40] I. V. Lerner and Yu. E. Lozovik, Zh. Eksp. Teor. Fiz. (Leningrad) **80**, 1488 (1981) [Sov. Phys. JETP **53**, 763 (1981)].
[41] A. B. Dzyubenko and Yu. E. Lozovik, Fiz. Tverd. Tela (Leningrad) **25**, 159 (1983) [Sov. Phys. Solid State **25**, 874 (1983)]; **26**, 1540 (1984) [**26**, 938 (1984)].
[42] D. Paquet, T. M. Rice, and K. Ueda, Phys. Rev. B **32**, 5208 (1985).
[43] A. Bychkov and E. I. Rashba, Phys. Rev. B **44**, 6212 (1991).
[44] S. Schmitt-Rink, Festkörperprobleme **31**, 247 (1991).
[45] A. B. Dzyubenko and Yu. E. Lozovik, J. Phys. A **24**, 415 (1991).